Preclinical Comparison of the ^{64}Cu- and ^{68}Ga-Labeled GRPR-Targeted Compounds RM2 and AMTG, as Well as First-in-Humans [^{68}Ga]Ga-AMTG PET/CT

Lena Koller[1], Markus Joksch[2], Sarah Schwarzenböck[2], Jens Kurth[2], Martin Heuschkel[2], Nadine Holzleitner[1], Roswitha Beck[1], Gunhild von Amsberg[3], Hans-Jürgen Wester[1], Bernd Joachim Krause*[2], and Thomas Günther*[1]

[1]*Pharmaceutical Radiochemistry, Technical University of Munich, Garching, Germany;* [2]*Department of Nuclear Medicine, Rostock University Medical Center, Rostock, Germany; and* [3]*Department of Oncology, University Medical Center Hamburg–Eppendorf, Hamburg, Germany*

Despite the recent success of prostate-specific membrane antigen (PSMA)–targeted compounds for theranostic use in prostate cancer (PCa), alternative options for the detection and treatment of PSMA-negative lesions are needed. We have recently developed a novel gastrin-releasing peptide receptor (GRPR) ligand with improved metabolic stability, which might improve diagnostic and therapeutic efficacy and could be valuable for PSMA-negative PCa patients. Our aim was to examine its suitability for theranostic use. We performed a comparative preclinical study on [^{64}Cu]Cu-/[^{68}Ga]Ga-AMTG ([^{64}Cu]Cu-/[^{68}Ga]Ga-α-Me-L-Trp^{8}-RM2) using [^{64}Cu]Cu-/[^{68}Ga]Ga-RM2 ([^{64}Cu]Cu-/[^{68}Ga]Ga-DOTA-Pip^{5}-Phe^{6}-Gln^{7}-Trp^{8}-Ala^{9}-Val^{10}-Gly^{11}-His^{12}-Sta^{13}-Leu^{14}-NH_2) as a reference compound and investigated [^{68}Ga]Ga-AMTG in a proof-of-concept study in a PCa patient. **Methods:** Peptides were labeled with ^{64}Cu (80 °C, 1.0 M NaOAc, pH 5.50) and ^{68}Ga (90 °C, 0.25 M NaOAc, pH 4.50). GRPR affinity (half-maximal inhibitory concentration, room temperature, 2 h) and GRPR-mediated internalization (37 °C, 60 min) were examined on PC-3 cells. Biodistribution studies were performed at 1 h after injection in PC-3 tumor–bearing mice. For a first-in-humans application, 173 MBq of [^{68}Ga]Ga-AMTG were administered intravenously and whole-body PET/CT scans were acquired at 75 min after injection. **Results:** ^{64}Cu- and ^{68}Ga-labeling proceeded almost quantitatively (>98%). All compounds revealed similarly high GRPR affinity (half-maximal inhibitory concentration, 1.5–4.0 nM) and high receptor-bound fractions (79%–84% of cell-associated activity). In vivo, high activity levels (percentage injected dose per gram) were found in the PC-3 tumor (14.1–15.1 %ID/g) and the pancreas (12.6–30.7 %ID/g), whereas further off-target accumulation was low at 1 h after injection, except for elevated liver uptake observed for both ^{64}Cu-labeled compounds. Overall biodistribution profiles and tumor-to-background ratios were comparable but slightly enhanced for the ^{68}Ga-labeled analogs in most organs. [^{68}Ga]Ga-AMTG confirmed the favorable pharmacokinetics—as evident from preclinical studies—in a patient with metastasized castration-resistant PCa showing intense uptake in several lesions. **Conclusion:** AMTG is eligible for theranostic use, as labeling with ^{64}Cu and ^{68}Ga, as well as ^{177}Lu (known from previous study), does not have a negative influence on its favorable biodistribution pattern. For this reason, further clinical evaluation is warranted.

Key Words: AMTG; first-in-humans; ^{68}Ga; ^{64}Cu; prostate cancer

J Nucl Med 2023; 64:1654–1659
DOI: 10.2967/jnumed.123.265771

Although prostate cancer (PCa) is associated with a high morbidity and mortality in metastasized castration-resistant PCa (mCRPC) (*1*), treatment has recently made some progress due to approval by the U.S. Food and Drug Administration and the European Medicines Agency of radioligand therapy (RLT) targeting the prostate-specific membrane antigen (PSMA) as a third-line therapy (*2,3*). However, in approximately 10%–20% of patients with recurrent PCa, a sufficiently high PSMA expression either is not present in PSMA-targeted PET imaging (*4,5*) or is lost in the course of subsequent treatment. Indeed, loss of PSMA expression may reflect aggressive transdifferentiation, a resistance mechanism to currently available standard therapies (*6,7*). In these patients, a PCa-atypical metastatic pattern is frequently observed (especially with visceral metastasis), whereas the classic adenocarcinoma features are often lost. Furthermore, PCa is known to be highly heterogeneous (*8*), which is why alternative compounds for imaging and RLT of PCa are required.

The gastrin-releasing peptide receptor (GRPR, bombesin-2 receptor) has been shown to be overexpressed in early, but more importantly in advanced and aggressive, PCa (*9,10*). Moreover, PCa patient cohorts that underwent both PSMA and GRPR PET revealed some metastases that were found only by the PSMA-targeted compound and others that were detected only by the GRPR-targeted compound; a complementary role for these targets in PCa is therefore anticipated (*11–14*). The GRPR-targeted radiopharmaceutical most often clinically applied, [^{68}Ga]Ga-RM2 ([^{68}Ga]Ga-DOTA-Pip^{5}-Phe^{6}-Gln^{7}-Trp^{8}-Ala^{9}-Val^{10}-Gly^{11}-His^{12}-Sta^{13}-Leu^{14}-NH_2), displayed favorable biodistribution patterns in humans, as high activity levels were found only in tumor lesions and the pancreas (*11,15,16*). Hence, its ^{177}Lu-labeled analog was used for RLT in PSMA-negative/GRPR-positive PCa patients, and this analog demonstrated promising dosimetry data (*17*). However, the limited metabolic stability of [^{68}Ga]Ga-RM2 has been discussed (*18*), being the motivation for our group to develop a RM2 derivative,

Received Mar. 24, 2023; revision accepted Jun. 12, 2023.
For correspondence or reprints, contact Thomas Günther (thomas.guenther@tum.de)
*Contributed equally to this work.
Published online Jul. 20, 2023.

[^{177}Lu]Lu-AMTG ([^{177}Lu]Lu-α-Me-L-Trp^{8}-RM2), which retained the favorable pharmacokinetics of [^{68}Ga]Ga-/[^{177}Lu]Lu-RM2 but showed distinctly increased metabolic stability in vivo and could thus improve therapeutic efficacy (*19*).

To confirm a sufficient GRPR expression on PCa cells before GRPR RLT, imaging of preferably PSMA-negative PCa patients is required first, which is why, with regard to a potential RLT using [^{177}Lu]Lu-AMTG, it would be advantageous to have a pendant for PET imaging. Due to the presence of a DOTA chelator, the use of the established theranostic pair ^{68}Ga and ^{177}Lu is well feasible. Besides ^{68}Ga, ^{64}Cu has recently emerged as an interesting alternative for PET imaging because of its longer half-life (12.7 h) and positron energy ($E_{\beta+,max}$, 653 keV), which is similar to the positron energy of ^{18}F and thus enables a high spatial resolution in PET despite its low positron decay probability of approximately 17% (*20*).

Hence, this study aimed to elucidate whether the AMTG peptide, originally designed for RLT, could also be used for PET imaging when labeled with either ^{64}Cu or ^{68}Ga. A comparative preclinical evaluation on [^{64}Cu]Cu-/[^{68}Ga]Ga-AMTG and [^{64}Cu]Cu-/[^{68}Ga]Ga-RM2 encompassed the determination of GRPR affinity (half-maximal inhibitory concentration [IC_{50}]) and GRPR-mediated internalization on PC-3 cells, lipophilicity (as evaluated by *n*-octanol/phosphate-buffered saline solution distribution coefficient distribution coefficients at pH 7.4 [log$D_{7.4}$]), and biodistribution in PC-3 tumor–bearing mice. Moreover, we selected [^{68}Ga]Ga-AMTG for clinical translation in a first-in-humans PET/CT examination in a patient with mCRPC.

MATERIALS AND METHODS

Chemical Synthesis and Labeling Procedures

A detailed description of the precursor synthesis is provided in the supplemental materials (available at http://jnm.snmjournals.org). Purification was accomplished via reversed-phase high-performance liquid chromatography (HPLC).

^{64}Cu and ^{68}Ga labeling was performed in analogy to an established protocol for ^{177}Lu labeling (*19*). A detailed description of the labeling procedures is provided in the supplemental materials. [^{64}Cu]$CuCl_2$ was purchased from DSD-Pharma GmbH. [^{68}Ga]$GaCl_3$ was provided by ITM Isotope Technologies Munich SE. The radiolabeled reference, *3*-[^{125}I]I-Tyr^{6}-MJ9 (Supplemental Fig. 1), was prepared according to reported procedures (*19,21*). Characterization of all GRPR ligands is provided in Supplemental Figures 2–4.

The synthesis of [^{68}Ga]Ga-AMTG according to good manufacturing practices for human PET/CT studies was performed using a good radiopharmaceutical practice module (Scintomics GmbH) while using an SC-01 gallium peptide labeling kit (ABX). [^{68}Ga]$GaCl_3$ was obtained from a GalliaPharm generator (Eckert & Ziegler) and was trapped on a PS-H^+ cartridge (ABX), which was eluted by a sodium chloride solution. The eluate was transferred in the reactor containing the AMTG precursor and the 4-(2-hydroxyethyl)-1-piperazineethanesulfonic acid (HEPES) buffer. The solution was heated and afterward transferred to a Sep-Pak C18 Light cartridge (Waters) for purification. After washing with water, the cartridge was eluted with ethanol and the solution was diluted with phosphate-buffered saline. The Cathivex-GV (Merck KGaA) was used as a sterile filter after the synthesis. Quality control included an instant thin-layer chromatography silica gel scan (NH_4OAc/MeOH; Agilent), as well as an HPLC measurement against the corresponding reference compound, [^{nat}Ga]Ga-AMTG. Compliance with the HEPES limit was determined by a spot test. Furthermore, a sterile filter integrity test, a limulus amebocyte lysate test, and a postapplication sterility test were performed. The ethanol concentration was measured by gas chromatography analysis.

In Vitro Experiments

All in vitro experiments (IC_{50} and log$D_{7.4}$) were performed according to a previously published procedure (*19*). A detailed description is provided in the supplemental materials.

In Vivo Experiments

Animal Experiments. All animal experiments were conducted according to a previously published protocol (*19*) and in accordance with general animal welfare regulations in Germany (German animal protection act, in the edition of the announcement dated May 18, 2006, as amended by article 280 of June 19, 2020, approval ROB-55.2-1-2532.Vet_02-18-109 by the General Administration of Upper Bavaria) and the institutional guidelines for the care and use of animals. Exclusion criteria for animals from an experiment were weight loss of more than 20%, a tumor size of more than 1,500 mm^3, ulceration of the tumor, respiratory distress, or a change in behavior. None of these criteria applied to any animal from the experiment. Neither randomization nor masking was applied in the allocation of the experiments. The health status of the animals was specific pathogen-free according to the recommendation of the Federation of European Laboratory Animal Science Associations. The study was performed in compliance with the ARRIVE guidelines (Animal Research: Reporting of In Vivo Experiments).

For biodistribution studies, approximately 2–4 MBq (100 pmol, 150 μL) of the ^{64}Cu-/^{68}Ga-labeled GRPR ligand were injected into the tail vein of anesthetized (2% isoflurane) 2- to 3-mo-old female PC-3 tumor–bearing CB17-SCID mice (n = 4). Organs were removed and weighed, and radioactivity was measured in a γ-counter (Perkin Elmer) after euthanasia at 1 h after injection.

Acquired data were statistically analyzed via a Student *t*-test via Excel (Microsoft Corp.) and OriginPro software (version 9.7) from OriginLab Corp. Acquired P values of less than 0.05 were considered statistically significant.

PET/CT in Patient. [^{68}Ga]Ga-AMTG was applied as an individual medical diagnostic test in a 72-y-old patient with advanced-stage mCRPC for whom no other diagnostic or therapeutic options were available. This use is allowed by the German Medical Act (§13 2b Arzneimittelgesetz), which waives the need for institutional review board approval. The legal and ethical compliance of this approach has recently been reviewed by the local ethics committee in the context of requesting approval for retrospective evaluation of therapy data obtained in this way (Ethics Committee at Rostock University, file no. A 2018-0240). The patient gave written informed consent after receiving comprehensive medical information from a board-certified nuclear medicine physician. The anonymized analyses were performed in accordance with the Declaration of Helsinki and its later amendments and with the legal considerations of clinical guidelines.

A detailed description of the patient's history is provided in the supplemental materials. The patient underwent [^{68}Ga]Ga-AMTG whole-body PET/CT using a Gemini TF 16 (Philips Healthcare) at 75 min after injection of 173 MBq of [^{68}Ga]Ga-AMTG. Whole-body CT imaging was performed as auxiliary CT (120 kVp, 40 mAs). PET datasets were reconstructed using the blob ordered-subsets time-of-flight protocol (3 iterations, 31 subsets), corrected for randoms, scatter, decay, and attenuation (using whole-body auxiliary CT).

RESULTS

Synthesis and Radiolabeling

Manual synthesis of RM2 and AMTG yielded 14% and 12% labeling precursor, respectively, after purification by reversed-phase HPLC (chemical purity > 98%, determined by reversed-phase

HPLC at λ = 220 nm). Complexation of all ligands with a 2.5-fold excess of [^{nat}Ga]Ga(NO_3)$_3$ and [^{nat}Cu]$CuCl_2$ each resulted in quantitative yields. The radiolabeled reference, 3-[^{125}I]I-Tyr^6-MJ9, was produced in a radiochemical yield and purity of 29% and more than 98%, respectively, after reversed-phase HPLC purification. Both ^{64}Cu- and ^{68}Ga-labeling was performed manually, each resulting in radiochemical yields and purities of more than 98% as well as molar activities of 55 ± 4 GBq/μmol (decay-corrected) and 35 ± 3 GBq/μmol (decay-corrected). Both ^{64}Cu- and ^{68}Ga-labeled RM2, as well as AMTG, were used without further purification.

The synthesized batch used for the patient yielded 409 MBq (~56% non–decay-corrected). All specifications were fulfilled. The pH of the 16 mL of solution was 7. The reference compound and the radiolabeled product displayed the same HPLC retention times. The radiochemical purity determined by HPLC was 98.7%, and the content of unbound [^{68}Ga]Ga-species was less than 0.3%. Thin-layer chromatography measurement was in line with less than 0.5% of unbound [^{68}Ga]Ga^{3+}.

In Vitro Characterization

The ^{nat}Cu- and ^{nat}Ga-labeled compounds exhibited high GRPR affinity on PC-3 cells, with IC_{50} values in the range of 1.5–4.0 nM (Fig. 1A; Supplemental Table 1; Supplemental Fig. 5). Although overall internalization was low for all GRPR ligands, the more affine ^{68}Ga-labeled compounds were internalized significantly higher within 1 h by PC-3 cells than were their ^{64}Cu-labeled counterparts ($P < 0.04$, Fig. 1B). It was evident for all analogs that a higher GRPR affinity led to increased internalized (Fig. 2A), as well as receptor-bound noninternalized, fractions (Fig. 2B), which is why the ratio of receptor-bound to internalized fraction was nearly constant, regardless of their GRPR affinity (Fig. 2C). Log$D_{7.4}$ was similar for all compounds (Fig. 1C). However, the ^{68}Ga-labeled ligands exhibited significantly lower lipophilicity than their ^{64}Cu-labeled analogs ($P < 0.01$).

In Vivo Characterization

In vivo studies on PC-3 tumor–bearing mice at 1 h after injection (Fig. 3; Supplemental Table 2) revealed favorable biodistribution profiles with similarly low off-target accumulation for ^{64}Cu- and ^{68}Ga-labeled RM2 and AMTG in most organs. Although the highest uptake values were determined for all derivatives in the tumor (14.1%–15.1% injected dose per gram [%ID/g]) and the pancreas (12.6–30.7 %ID/g), significantly increased accumulation was observed for the ^{64}Cu-labeled analogs in the heart and the lung as compared with their ^{68}Ga-labeled counterparts ($P < 0.003$). Moreover, activity levels in the liver were distinctly enhanced for the ^{64}Cu-labeled compounds ($P < 0.001$). Uptake values were elevated in the pancreas for the ^{68}Ga-labeled analogs as compared with the ^{64}Cu-labeled analogs ($P < 0.05$). Accumulation in the adrenals was significantly higher for [^{64}Cu]Cu-/[^{68}Ga]Ga-AMTG than for [^{64}Cu]Cu-/[^{68}Ga]Ga-RM2 ($P < 0.03$) yet was on a very low level (1.9–2.8 vs. 1.0–1.1 %ID/g).

In general, tumor-to-background (T/B) ratios for the ^{68}Ga-labeled compounds were higher than for the ^{64}Cu-labeled derivatives (Fig. 4; Supplemental Table 3). Both [^{64}Cu]Cu-AMTG and [^{64}Cu]Cu-RM2 showed similar T/B ratios, except in the adrenals and kidneys, in which the ratio for the latter was slightly higher. Although [^{68}Ga]Ga-AMTG displayed enhanced T/B ratios in the muscle and the bone, [^{68}Ga]Ga-RM2 demonstrated higher T/B ratios in the spleen, the liver, and the adrenals. Because overall biodistribution patterns were comparable for both ^{68}Ga-labeled GRPR ligands, and [^{68}Ga]Ga-RM2 had already been applied in clinical studies, we selected [^{68}Ga]Ga-AMTG for PET imaging in a first-in-humans application.

Proof-of-Concept Study in Patient

[^{68}Ga]Ga-AMTG PET showed a favorable biodistribution, with uptake being highest in tumor lesions and the pancreas. Besides the bladder (because of excretion), no significant activity levels were found in other organs. One month previously, the patient had undergone [^{18}F]F-PSMA-1007 PET/CT, which showed only 1 subphrenic lesion with low [^{18}F]F-PSMA-1007 uptake (Fig. 5A; Supplemental Fig. 7). On [^{68}Ga]Ga-AMTG PET/CT, multiple lesions with intense focal uptake could be detected in the peritoneum, the subphrenic area adjacent to the liver, and between the left internal and external iliac arteries; these [^{68}Ga]Ga-AMTG–positive findings corresponded to soft-tissue lesions that were visualized on CT (Fig. 5B; Supplemental Fig. 7).

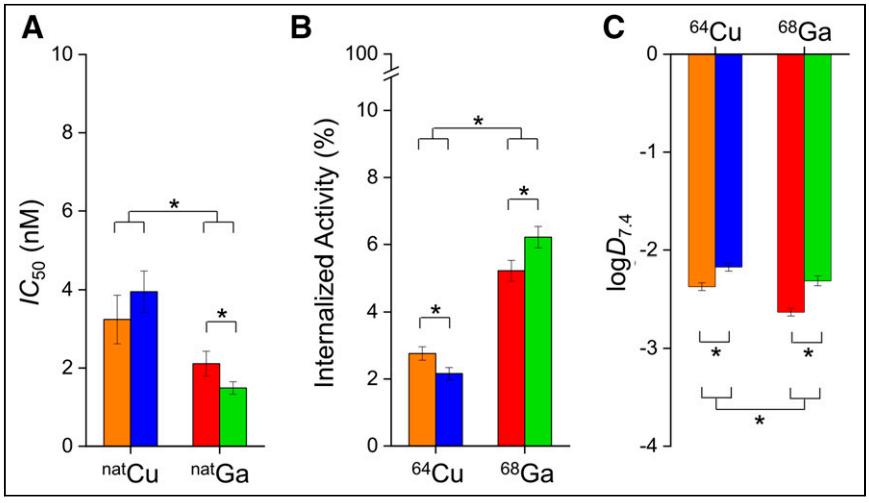

FIGURE 1. In vitro data of [$^{nat/64}$Cu]Cu-RM2 (orange), [$^{nat/68}$Ga]Ga-RM2 (red), [$^{nat/64}$Cu]Cu-AMTG (blue), and [$^{nat/68}$Ga]Ga-AMTG (green). Data are expressed as mean ± SD. (A) Affinity data on PC-3 cells (1.5×10^5 cells/mL/well) using 3-[^{125}I]I-Tyr^6-MJ9 (0.2 nM/well) as radiolabeled reference (2 h, room temperature, Hanks balanced salt solution plus 1% bovine serum albumin, *v/v*). (B) GRPR-mediated internalization (1.0 nM/well) on PC-3 cells as percentage of applied activity (incubation at 37 °C for 1 h, Dulbecco modified Eagle medium/F-12 plus 5% bovine serum albumin [*v/v*], 1.5×10^5 cells/mL/well). Data are corrected for nonspecific binding (10^{-3} M [^{nat}Lu]Lu-RM2). (C) Log$D_{7.4}$. *$P < 0.05$.

DISCUSSION

Based on the need for treatment options for PSMA-negative PCa patients, alternative targets such as the GRPR may become more relevant. We recently developed [^{177}Lu]Lu-AMTG, an RM2 derivative with noticeably increased metabolic stability in vivo (*19*), initially for an improved GRPR RLT. Because we additionally wanted to explore its potential for PET imaging, we performed a preclinical study on [^{64}Cu]Cu-/[^{68}Ga]Ga-AMTG and a first-in-humans application using [^{68}Ga]Ga-AMTG.

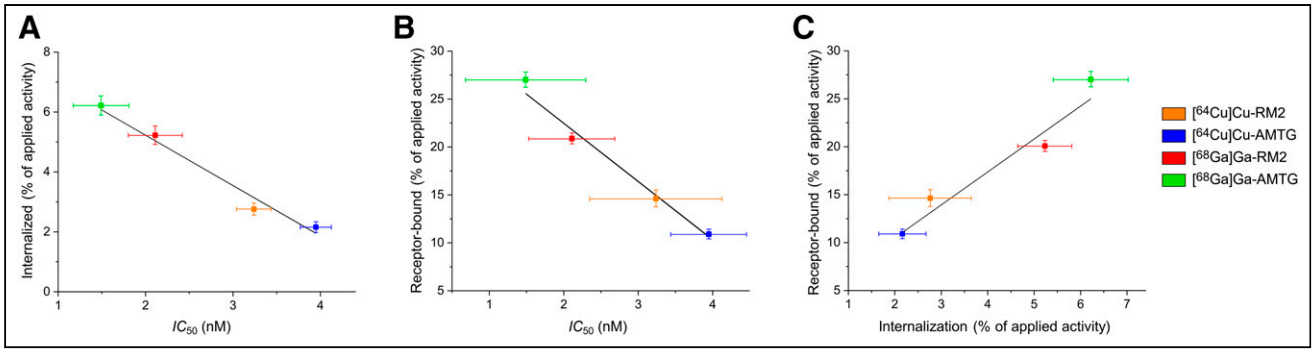

FIGURE 2. Internalization data of [^{64}Cu]Cu-RM2, [^{64}Cu]Cu-AMTG, [^{68}Ga]Ga-RM2, and [^{68}Ga]Ga-AMTG. Data are expressed as mean ± SD. (A) Ratio of IC_{50} and internalized fraction. (B) Ratio of IC_{50} and receptor-bound, noninternalized fraction. (C) Ratio of internalized and receptor-bound, noninternalized fraction.

Synthesis of the precursors was easily accessible via solid-phase peptide synthesis, and complexation with $^{nat/64}$Cu and $^{nat/68}$Ga proceeded quantitatively. The ^{nat}Cu- and ^{nat}Ga-labeled compounds were not purified before affinity studies, as we could show in a previous study that an excess of ions, such as Lu^{3+}, did not have any influence on GRPR affinity (*19*). Because of their structural similarity, all 4 compounds revealed comparably high GRPR affinity (IC_{50}, 1.5–4.0 nM), which met or even surpassed the values of their $^{nat/177}$Lu-labeled counterparts (IC_{50}, 3.0–3.5 nM) (*19*). The high receptor-bound fractions (79%–84% of cell-associated activity) found for all 4 analogs corroborated well with the values determined for [^{177}Lu]Lu-AMTG/RM2 (*19*) and are generally expected for antagonists (*22*). The log$D_{7.4}$ of the 4 compounds was in a range (−2.6 to −2.2) comparable to that of the previously published ^{177}Lu-labeled analogs (*19*).

Because we could show that a change in the radionuclide (^{64}Cu and ^{68}Ga instead of ^{177}Lu) had minimal impact on in vitro parameters, we expected in vivo properties similar to those of the previously reported [^{177}Lu]Lu-AMTG/RM2 (*19*). Indeed, the overall biodistribution profiles of [^{64}Cu]Cu-/[^{68}Ga]Ga-AMTG and [^{64}Cu]Cu-/[^{68}Ga]Ga-RM2 at 1 h after injection displayed high activity levels in the tumor and pancreas, whereas further off-target accumulation was either low or cleared rapidly within the first hour after injection. An exception was the liver, which revealed increased activity levels for the ^{64}Cu-labeled compounds as compared with the ^{68}Ga-labeled compounds. This increase was expected, since there are reports on the insufficient in vivo stability of the Cu-DOTA chelate (*23–25*), which led to a significant removal of ^{64}Cu from the DOTA chelator via transchelation to the superoxide dismutase in the liver and storage of free $^{64}Cu^{2+}$ ions in hepatocytes by metallothionein 1 and 2 (*26*). The instability of the ^{64}Cu-DOTA chelate could also explain the generally decreased T/B ratios of the ^{64}Cu-labeled ligands as compared with the ^{68}Ga-labeled ligands because of the thus higher off-target accumulation in most organs at 1 h after injection.

However, the high in vivo instability of the Cu-DOTA chelate in mice cannot be directly transferred to the human situation, because metabolism between these species is noticeably different. For example, high activity levels (~6 %ID/g) were found in the murine liver at 1 h after injection of [^{64}Cu]Cu-DOTATATE (*25*), whereas in humans slightly elevated activity levels observed in the liver did not hamper the detection of a variety of liver metastases (*27–29*). Dosimetry studies on [^{64}Cu]Cu-DOTATATE in 5 patients revealed that the dose delivered to the liver was similar to that delivered to the kidneys (0.161 vs. 0.139 Gy/GBq) (*27*), and this dose is indeed 2- to 4-fold higher than for [^{68}Ga]Ga-DOTATATE (0.045 and 0.092 Sv/GBq, respectively) but does not affect its clinical use (*30*).

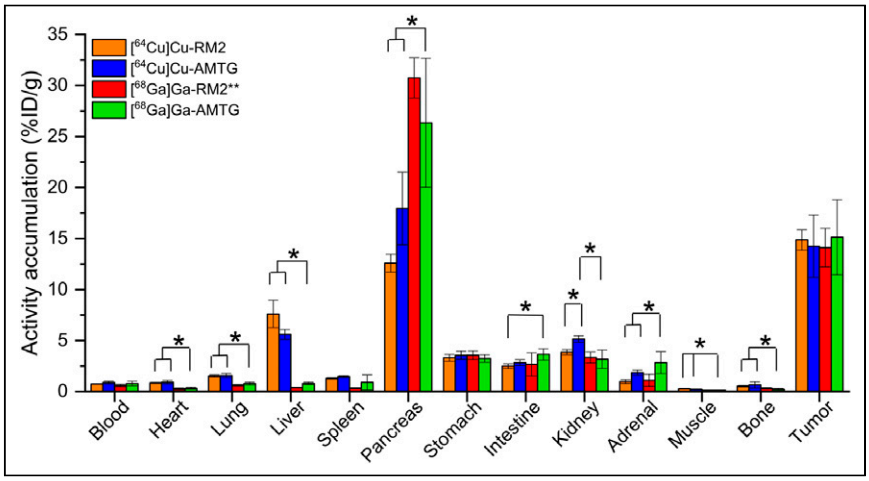

FIGURE 3. Biodistribution data of [^{64}Cu]Cu-RM2, [^{64}Cu]Cu-AMTG, [^{68}Ga]Ga-RM2, and [^{68}Ga]Ga-AMTG in selected organs at 1 h after injection in PC-3 tumor–bearing CB17-SCID mice (100 pmol each). Data are expressed as %ID/g, mean ± SD (n = 4). *P < 0.05. **10 pmol, NMRI nu/nu-mice, data taken from Mansi et al. (*31*). Statistical comparison with regard to [^{68}Ga]Ga-RM2 not applicable.

[^{68}Ga]Ga-AMTG (100 pmol, CB17-SCID mice) displayed a similar biodistribution profile (Supplemental Fig. 6) and thus comparable T/B ratios in most organs to the clinical standard for PET imaging of GRPR-expressing malignancies, [^{68}Ga]Ga-RM2 (10 pmol, NMRI nu/nu-mice, data taken from Mansi et al. (*31*)). The comparison of these 2 tracers is a limitation of this study, as biodistribution studies of [^{68}Ga]Ga-RM2 have been performed by another group using different mouse models and precursor amounts than we did for [^{68}Ga]Ga-AMTG. Because preclinical data, particularly overall pharmacokinetics, were mainly comparable for [^{64}Cu]Cu-/[^{68}Ga]Ga-AMTG and [^{64}Cu]Cu-/[^{68}Ga]Ga-RM2, both AMTG derivatives appear to be promising candidates for clinical translation. Although [^{68}Ga]Ga-AMTG

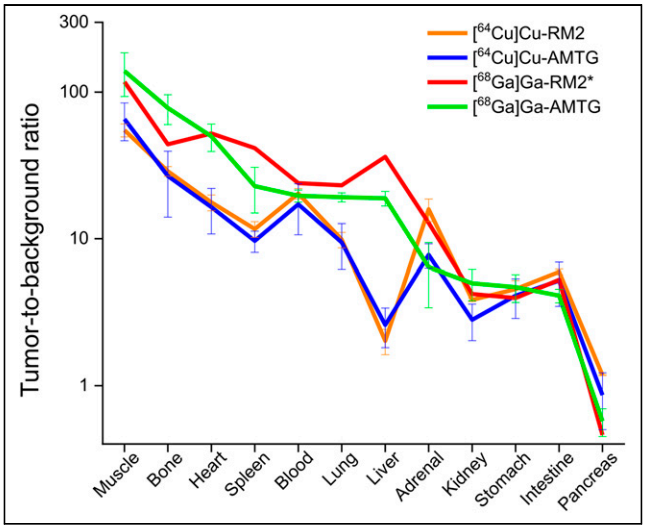

FIGURE 4. Graphical comparison of T/B ratios for selected organs for [^{64}Cu]Cu-RM2, [^{64}Cu]Cu-AMTG, [^{68}Ga]Ga-RM2, and [^{68}Ga]Ga-AMTG. Biodistribution studies were performed at 1 h after injection in PC-3 tumor–bearing CB17-SCID mice (100 pmol each). Data are expressed as mean ± SD (n = 4). *10 pmol, NMRI nu/nu-mice, data taken from Mansi et al. (*31*)

was selected for a first-in-humans investigation in a PCa patient, ^{64}Cu-labeled compounds might be superior to ^{68}Ga-labeled compounds in the future because of the longer half-life of ^{64}Cu (12.7 vs. 67.6 min), which would enable PET imaging over an extended time span. In addition, its lower positron energy ($E_{\beta+,max}$, 653 vs. 1,899 keV) allows for a higher resolution in PET (*20*). However, it remains to be seen whether the low positron decay probability of ^{64}Cu generates some drawbacks for PET imaging, such as with regard to counting statistics. Moreover, the current availability of ^{68}Ga (generator) is a significant advantage over ^{64}Cu (cyclotron).

For a first-in-humans application, good-manufacturing-practice synthesis of [^{68}Ga]Ga-AMTG was achieved within 36 min, yielded 409 MBq (~56% non–decay-corrected), and fulfilled all specifications (clear and particle-free solution, pH 7, radiochemical purity > 98%, unbound [^{68}Ga]Ga^{3+} ≤ 0.5%, HEPES limit, ethanol concentration, endotoxin limit, filter integrity).

[^{68}Ga]Ga-AMTG revealed a favorable biodistribution in a PET/CT scan of an mCRPC patient at 75 min after injection, with high uptake in tumor lesions and the pancreas, whereas further off-target accumulation was low. Moreover, [^{68}Ga]Ga-AMTG PET/CT revealed distinctly more lesions and increased SUVs than [^{18}F]F-PSMA-1007 in this mCRPC patient. An epithelial–mesenchymal transition is expected in PCa after several treatment lines including PSMA-targeted RLT (*32*), can lead to a loss of PSMA expression, and thus requires alternative treatment options. For such patients, GRPR-targeted compounds could offer an alternative option for imaging and RLT. The feasibility of [^{68}Ga]Ga-AMTG for such cases has been shown for only 1 patient to date—a limitation of this study and why further clinical evaluation has to be performed to confirm this promising preliminary result. Because [^{68}Ga]Ga-AMTG PET did not display noticeable uptake in organs other than the pancreas, and because pancreatic clearance is known to occur within the first hours after injection, this could open new possibilities for treatment of PCa, provided that GRPR expression is sufficient. Moreover, unlike PSMA inhibitors, GRPR-targeted compounds do not accumulate in the salivary glands and the kidneys, among others, which is why the use of ^{90}Y or α-particle–emitting radionuclides likely causes less severe side effects.

CONCLUSION

Both [^{64}Cu]Cu- and [^{68}Ga]Ga-AMTG revealed excellent preclinical data and might be valuable tools for PET imaging of PSMA-negative PCa in progressed disease stages, as well as in other cancer types such as breast cancer and glioblastoma multiforme. A first-in-humans examination in an mCRPC patient displayed favorable biodistribution patterns and did not show any biosafety issues or significant differences from the clinically established reference, [^{68}Ga]Ga-RM2. [^{68}Ga]Ga-AMTG PET/CT identified noticeably more lesions than [^{18}F]F-PSMA-1007, likely due to an aggressive transdifferentiation of PCa and, thus, limited PSMA expression. Because an enhanced in vivo stability was observed in previous studies for the AMTG peptide, an improved RLT might be achievable in these patients, rendering this peptide a valuable theranostic tool. Further patient studies will elucidate whether these promising results are reflected on a broader scale.

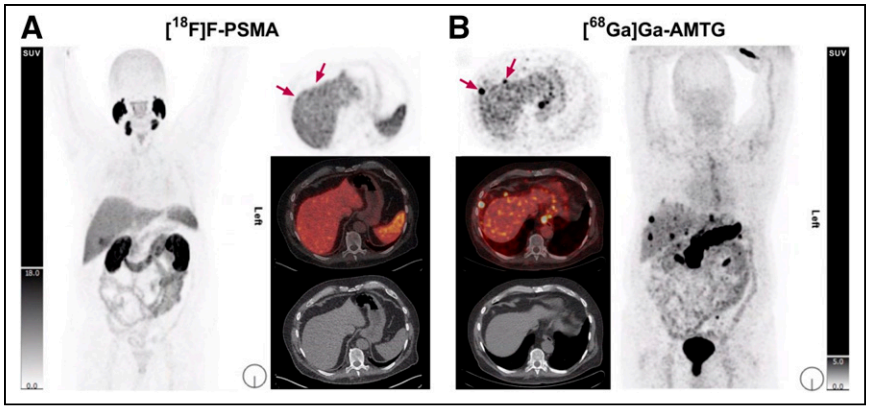

FIGURE 5. Patient with mCRPC after 4 cycles of [^{177}Lu]Lu-PSMA-617 RLT, with multiple small perihepatic and abdominal lymph node metastases that currently show no or only faint uptake on [^{18}F]F-PSMA-1007 PET/CT. (A) Left: PET maximum-intensity projection. Upper right: transaxial [^{18}F]F-PSMA-1007 PET. Middle right: transaxial fused PET/CT. Lower right: transaxial CT but intense uptake on [^{68}Ga]Ga-AMTG PET/CT. (B) Right: PET maximum-intensity projection. Upper left: transaxial [^{68}Ga]Ga-AMTG PET. Middle left: transaxial fused PET/CT. Lower left: transaxial CT.

DISCLOSURE

A patent application on modified GRPR-targeted ligands including AMTG, with Thomas Günther and Hans-Jürgen Wester as inventors, has been filed. Hans-Jürgen Wester is founder and shareholder of Scintomics GmbH. Bernd Joachim Krause is an advisor for Terumo, Rotop, AAA/Novartis, PSI CRO, ITM, Bayer, and Janssen; receives third-party funding from AAA/Novartis, AMGEN, and Eisai; receives travel support from AAA/Novartis; and receives royalties from AAA/Novartis, Bayer, and Janssen.

No other potential conflict of interest relevant to this article was reported.

KEY POINTS

QUESTION: Is the metabolically more stable peptide AMTG (as compared with RM2)—particularly designed for an improved RLT of GRPR-expression malignancies—also an option for imaging applying ^{64}Cu or ^{68}Ga?

PERTINENT FINDINGS: [^{64}Cu]Cu-/[^{68}Ga]Ga-AMTG and [^{64}Cu]Cu-/[^{68}Ga]Ga-RM2 displayed comparable pharmacokinetics preclinically, and [^{68}Ga]Ga-AMTG clinically, to those of the often used [^{68}Ga]Ga-RM2, rendering the AMTG peptide a promising theranostic tool for PET imaging and RLT.

IMPLICATIONS FOR PATIENT CARE: Although the clinical value of [^{64}Cu]Cu- and [^{68}Ga]Ga-AMTG (and [^{177}Lu]Lu-AMTG) has to be further elucidated, this study might pave the way for clinical use of an improved theranostic peptide and, thus, patient care.

REFERENCES

1. Prostate cancer prognosis. Johns Hopkins Medicine website. https://www.hopkinsmedicine.org/health/conditions-and-diseases/prostate-cancer/prostate-cancer-prognosis. Accessed June 30, 2023.
2. Sartor O, de Bono J, Chi KN, et al. Lutetium-177-PSMA-617 for metastatic castration-resistant prostate cancer. *N Engl J Med.* 2021;385:1091–1103.
3. FDA approves Pluvicto for metastatic castration-resistant prostate cancer. U.S. Food and Drug Administration website. https://www.fda.gov/drugs/resources-information-approved-drugs/fda-approves-pluvicto-metastatic-castration-resistant-prostate-cancer. Revised March 23, 2022. Accessed June 30, 2023.
4. Afshar-Oromieh A, Holland-Letz T, Giesel FL, et al. Diagnostic performance of ^{68}Ga-PSMA-11 (HBED-CC) PET/CT in patients with recurrent prostate cancer: evaluation in 1007 patients. *Eur J Nucl Med Mol Imaging.* 2017;44:1258–1268.
5. Eiber M, Maurer T, Souvatzoglou M, et al. Evaluation of hybrid ^{68}Ga-PSMA ligand PET/CT in 248 patients with biochemical recurrence after radical prostatectomy. *J Nucl Med.* 2015;56:668–674.
6. Hofman MS, Emmett L, Sandhu S, et al. TheraP: ^{177}Lu-PSMA-617 (LuPSMA) versus cabazitaxel in metastatic castration-resistant prostate cancer (mCRPC) progressing after docetaxel—overall survival after median follow-up of 3 years (ANZUP 1603) [abstract]. *J Clin Oncol.* 2022;40(suppl):5000.
7. Merkens L, Sailer V, Lessel D, et al. Aggressive variants of prostate cancer: underlying mechanisms of neuroendocrine transdifferentiation. *J Exp Clin Cancer Res.* 2022;41:46.
8. Macintosh CA, Stower M, Reid N, Maitland NJ. Precise microdissection of human prostate cancers reveals genotypic heterogeneity. *Cancer Res.* 1998;58:23–28.
9. Maina T, Bergsma H, Kulkarni HR, et al. Preclinical and first clinical experience with the gastrin-releasing peptide receptor-antagonist [^{68}Ga]SB3 and PET/CT. *Eur J Nucl Med Mol Imaging.* 2016;43:964–973.
10. Reubi JC, Wenger S, Schmuckli-Maurer J, Schaer JC, Gugger M. Bombesin receptor subtypes in human cancers: detection with the universal radioligand ^{125}I-[D-TYR^{6}, beta-ALA^{11}, PHE^{13}, NLE^{14}] bombesin(6-14). *Clin Cancer Res.* 2002;8:1139–1146.
11. Baratto L, Song H, Duan H, et al. PSMA- and GRPR-targeted PET: results from 50 patients with biochemically recurrent prostate cancer. *J Nucl Med.* 2021;62:1545–1549.
12. Touijer KA, Michaud L, Alvarez HAV, et al. Prospective study of the radiolabeled GRPR antagonist BAY86-7548 for positron emission tomography/computed tomography imaging of newly diagnosed prostate cancer. *Eur Urol Oncol.* 2019;2:166–173.
13. Fassbender TF, Schiller F, Zamboglou C, et al. Voxel-based comparison of [^{68}Ga]Ga-RM2-PET/CT and [^{68}Ga]Ga-PSMA-11-PET/CT with histopathology for diagnosis of primary prostate cancer. *EJNMMI Res.* 2020;10:62.
14. Heuschkel M, Kurth J, Hakenberg OW, Nitsch S, Schwarzenböck SM, Krause BJ. Monocentric intraindividual comparison of ^{68}Ga-RM2 and ^{68}Ga-PSMA PET/CT in mCRPC [abstract]. *Eur J Nucl Med Mol Imaging.* 2019;46:526.
15. Stoykow C, Erbes T, Maecke HR, et al. Gastrin-releasing peptide receptor imaging in breast cancer using the receptor antagonist ^{68}Ga-RM2 and PET. *Theranostics.* 2016;6:1641–1650.
16. Baratto L, Duan H, Mäcke H, Iagaru A. Imaging the distribution of gastrin-releasing peptide receptors in cancer. *J Nucl Med.* 2020;61:792–798.
17. Kurth J, Krause BJ, Schwarzenböck SM, Bergner C, Hakenberg OW, Heuschkel M. First-in-human dosimetry of gastrin-releasing peptide receptor antagonist [^{177}Lu]Lu-RM2: a radiopharmaceutical for the treatment of metastatic castration-resistant prostate cancer. *Eur J Nucl Med Mol Imaging.* 2020;47:123–135.
18. Roivainen A, Kahkonen E, Luoto P, et al. Plasma pharmacokinetics, whole-body distribution, metabolism, and radiation dosimetry of ^{68}Ga bombesin antagonist BAY 86-7548 in healthy men. *J Nucl Med.* 2013;54:867–872.
19. Günther T, Deiser S, Felber V, Beck R, Wester HJ. Substitution of L-tryptophan by a-methyl-L-tryptophan in ^{177}Lu-RM2 results in ^{177}Lu-AMTG, a high-affinity gastrin-releasing peptide receptor ligand with improved in vivo stability. *J Nucl Med.* 2022;63:1364–1370.
20. Braune A, Oehme L, Freudenberg R, et al. Comparison of image quality and spatial resolution between ^{18}F, ^{68}Ga, and ^{64}Cu phantom measurements using a digital Biograph Vision PET/CT. *EJNMMI Phys.* 2022;9:58.
21. Nakagawa T, Hocart SJ, Schumann M, et al. Identification of key amino acids in the gastrin-releasing peptide receptor (GRPR) responsible for high affinity binding of gastrin-releasing peptide (GRP). *Biochem Pharmacol.* 2005;69:579–593.
22. Borgna F, Haller S, Rodriguez JMM, et al. Combination of terbium-161 with somatostatin receptor antagonists: a potential paradigm shift for the treatment of neuroendocrine neoplasms. *Eur J Nucl Med Mol Imaging.* 2022;49:1113–1126.
23. Boswell CA, Sun X, Niu W, et al. Comparative in vivo stability of copper-64-labeled cross-bridged and conventional tetraazamacrocyclic complexes. *J Med Chem.* 2004;47:1465–1474.
24. Persson M, El Ali HH, Binderup T, et al. Dosimetry of ^{64}Cu-DOTA-AE105, a PET tracer for uPAR imaging. *Nucl Med Biol.* 2014;41:290–295.
25. Rylova SN, Stoykow C, Del Pozzo L, et al. The somatostatin receptor 2 antagonist ^{64}Cu-NODAGA-JR11 outperforms ^{64}Cu-DOTA-TATE in a mouse xenograft model. *PLoS One.* 2018;13:e0195802.
26. Persson M, Hosseini M, Madsen J, et al. Improved PET imaging of uPAR expression using new ^{64}Cu-labeled cross-bridged peptide ligands: comparative in vitro and in vivo studies. *Theranostics.* 2013;3:618–632.
27. Pfeifer A, Knigge U, Mortensen J, et al. Clinical PET of neuroendocrine tumors using ^{64}Cu-DOTATATE: first-in-humans study. *J Nucl Med.* 2012;53:1207–1215.
28. Pfeifer A, Knigge U, Binderup T, et al. ^{64}Cu-DOTATATE PET for neuroendocrine tumors: a prospective head-to-head comparison with ^{111}In-DTPA-octreotide in 112 patients. *J Nucl Med.* 2015;56:847–854.
29. Johnbeck CB, Knigge U, Loft A, et al. Head-to-head comparison of ^{64}Cu-DOTATATE and ^{68}Ga-DOTATOC PET/CT: a prospective study of 59 patients with neuroendocrine tumors. *J Nucl Med.* 2017;58:451–457.
30. Walker RC, Smith GT, Liu E, Moore B, Clanton J, Stabin M. Measured human dosimetry of ^{68}Ga-DOTATATE. *J Nucl Med.* 2013;54:855–860.
31. Mansi R, Wang X, Forrer F, et al. Development of a potent DOTA-conjugated bombesin antagonist for targeting GRPr-positive tumours. *Eur J Nucl Med Mol Imaging.* 2011;38:97–107.
32. Hu CD, Choo R, Huang J. Neuroendocrine differentiation in prostate cancer: a mechanism of radioresistance and treatment failure. *Front Oncol.* 2015;5:90.